pp. 1–13 (2013)

Numerical simulation of blood flows with non-uniform distribution of erythrocytes and platelets

N. BESSONOV[*], E. BABUSHKINA[*], S. GOLOVASHCHENKO[†], A. TOSENBERGER[‡§], F. ATAULLAKHANOV[¶‖**††], M. PANTELEEV[¶‖**††], A. TOKAREV[¶‖], and V. VOLPERT[‡§‡‡]

Abstract — Blood cell interactions present an important mechanism in many processes occurring in blood. Due to different blood cell properties, cells of different types behave differently in the flow. Among the observed phenomena is segregation of erythrocytes, which group near the flow axis, from platelets, which migrate towards the blood vessel wall. In this work, a three dimensional model based on the Dissipative Particle Dynamics method is used to study the interaction of erythrocytes and platelets in a flow inside a cylindrical channel. Erythrocytes are modelled as elastic highly deformable membranes, while platelets are modelled as elastic spherical membranes which tend to preserve their spherical shape. As the result of the modelling, the separation of erythrocytes and platelets in a cylindrical vessel flow is shown for vessels of different diameters. Erythrocyte and platelet distribution profiles in the vessel cross-section are in good agreement with the existing experimental results. The described 3-D model can be used for further modelling of blood flow-related problems.

Physical interactions between red blood cells and platelets play an important role in the blood flow, and particularly in hemostasis and thrombosis [35,36]. In blood vessels with a diameter significantly larger than the diameter of an erythrocyte (around 8 μm), it is experimentally observed that erythrocytes, which occupy around 40% of

[*] Institute of Problems of Mechanical Engineering, Russian Academy of Sciences, Saint Petersburg 199178, Russia. Corresponding author. E-mail: nickbessonov@yahoo.com

[†] Manufacturing Systems Department, Ford Research Laboratory, 481214 Dearborn, USA

[‡] Institut Camille Jordan, UMR 5208 CNRS, University Lyon 1, 69622 Villeurbanne, France

[§] INRIA Team Dracula, INRIA Antenne Lyon la Doua 69603 Villeurbanne, France

[¶] National Research Center for Haematology Ministry of Healthcare of Russian Federation, Moscow 125167, Russia

[‖] Federal Research and Clinical Centre of Paediatric Haematology, Oncology and Immunology, Ministry of Healthcare of Russian Federation, Moscow 117198, Russia

[**] Faculty of Physics, M. V. Lomonosov Moscow State University, Moscow 119991, Russia

[††] Center for Theoretical Problems of Physicochemical Pharmacology, Russian Academy of Sciences, Moscow 119991, Russia

[‡‡] European Institute of Systems Biology and Medicine, 69007 Lyon, France

The study was supported by the Russian Foundation for Basic Research (Grants 10-01-91055, 11-04-00303, 11-04-12080, 12-04-00652, 12-04-00438, 12-04-32095, 12-04-33055, 14-01-91055), Russian Federation Presidential Scholarship for Young Scientists and Graduate Students and by the Russian Academy of Sciences Presidium Basic Research Programs for Molecular and Cellular Biology, Basic Science for Medicine, Integrative Physiology, and Molecular Mechanisms of Physiologic Functions, grants ANR Bimod, French–Russian project PICS, Mathematical Modelling of Blood Diseases, grant No. 14.740.11.0877 of the Ministry of Education and Research of the Russian Federation, Investigation of Spatial and Temporal Structures in Fluids with Applications to Mathematical Biology.

the blood volume, concentrate in the bulk of the flow (around the flow axis), while platelets are being pushed (migrate) towards the vessel wall. In the case of a vessel wall injury, this mechanism makes the process more efficient, as the platelets, which are crucial for hemostasis, are placed closer to the vessel wall and the injury site. In order to model and investigate more accurately the complex processes in blood, namely blood coagulation, it is important for the underlying model of the blood flow to capture the described behaviour and interactions of the blood cells.

Various methods have been used to model blood flows. We can split them into two main groups — continuous and discrete. Continuous models are based on mathematical knowledge of differential equations, where a flow is very accurately described by partial differential equations, generally the Navier–Stokes equations. In continuous models blood cells are considered in terms of their concentrations and are, therefore, also modelled by partial differential equations, which describe their motion via diffusion and convection [37, 41]. The disadvantage of this approach is that it does not describe the interaction between individual blood cells in the flow. Discrete models provide for the description of individual cells and their interactions. Such models are either based on the continuous description of a fluid flow, or their hydrodynamic properties have to be verified by comparison with continuous models. Erythrocytes are the most interesting and complex blood cells to model because of their deformability, and also because they constitute 95% of all cells in blood and occupy 40% of the blood volume. Therefore, most of the models of the blood flow, which are able to describe individual blood cells and their interactions, have been aimed to describe the motion of erythrocytes. They include erythrocyte membrane models and the results are compared to the known erythrocyte behaviour in different conditions. A particular form of behaviour is observed in a Poiseuille flow in a micro-channel where erythrocytes take the characteristic parachute shape. This aspect has been captured by both 2-D and 3-D Red Blood Cell (RBC) membrane models [9, 10, 16, 25, 28, 31, 40]. Other types of experimentally observed behaviour are RBC tumbling and tank-threading motion, as well as the erythrocyte response to stretching. Those properties have been successfully captured by 3-D erythrocyte membrane models [5, 7, 9, 10, 12, 17, 31]. All those types of behaviour are mainly related to a single erythrocyte in the flow. There are much fewer results on numerical simulation of several erythrocytes in a flow and their distribution.

Computational studies have been done in order to obtain such feature of the blood flow observed experimentally as the concentrated RBC core at the flow axis. Tsubota et al. [40] presented a two-dimensional particle model for the blood flow between two parallel rigid plates. The moving particle semi-explicit (MPS) method was used to analyze the blood plasma flow. An RBC was modelled as a deformable elastic membrane consisting of particles with elastic energy depending on the distance between the particles, the angle between the neighbouring elements, and conserving the area of the membrane. The simulation results demonstrated that RBCs are concentrating near the flow axis and form the cell-free layer near the boundaries. In the more recent work of Zhang et al. [43] another approach is used. A two-dimensional blood flow is simulated using the immersed-boundary lattice Boltz-

mann algorithm. Following Bagchi [3], RBCs are modelled as two-dimensional deformable biconcave membranes, while the inter-cellular interactions are modelled using the Morse potential. In addition to the presence of the cell-free layer it is shown that this layer's thickness increases with cell deformability. The known effect of erythrocytes migration toward the flow axis is observed, but platelets and their behaviour are not considered in these papers. AlMomani et al. [2] used the computational fluid dynamics (CFD) model to perform micro-scale simulations of platelet-RBC interactions in a shear flow. RBCs are assumed to be incompressible elliptical particles that retain their elliptical shape under deformation by imposed shear stresses, and platelets are assumed to be rigid particles of a circular shape. The interaction between neighbouring particles is due to repulsive forces from a 'soft' potential. It is shown in this paper that the concentration of platelets increases near the boundary, while erythrocytes are located near the flow axis. It was also found that platelets behaviour is affected by the relative differences in the size of platelets and RBCs, but not by the differences in shapes. The values of hematocrit were set to be 5%, 10%, and 15%, which are lower than the normal hematocrit level in blood. Furthermore, it was observed that the migratory effect is absent at low hematocrit values (e.g., Ht $= 5\%$), but occurs at higher values (e.g., Ht $= 10\%$) and becomes more evident as the hematocrit value increases. Another study [6] was devoted to a two-dimensional numerical investigation of the lateral platelet motion induced by RBCs. They used a combination of the lattice Boltzmann method for fluid motion and the Immersed Boundary method for the implementation of interaction between the fluid and the elastic objects suspended in or in contact with the fluid. A deformable elastic RBCs membrane was modelled following Skalak [34] approach, while platelets were modelled as approximately rigid circular objects. Simulations were carried out for the following values of hematocrit: 0%, 20%, and 40%. In the case of RBCs absence there was a negligible amount of lateral motion, however, it was clearly shown that a near-wall increase in the platelet concentration occurs rapidly (within the first 400 msec) for both 20% and 40% levels.

A major limitation of the works described above is consideration of the two-dimensional model of blood flow instead of the three-dimensional one. In contrast to these studies, our work represents the three-dimensional discrete model that includes simulation of blood as a suspension of erythrocytes and platelets in blood plasma. We have used the Dissipative Particle Dynamics (DPD) method to simulate the blood flow in a cylindrical vessel. DPD is a well developed and widely used approach to mesoscopic description of the fluid. RBCs are modelled as elastic highly deformable membranes. In contrast to [10,12], where a platelet is modelled as a rigid or almost rigid body, we consider a platelet as an elastic membrane. However, in our simulations the form of the platelets varies near the spherical shape. The advantage of such approach is the future possibility of developing a more complex platelet model and accounting for the platelet structure features. The main aim of this work is the investigation of RBCs and platelet interaction and the distribution of cells in the cross-section of the vessel. The blood flow was simulated for the vessels of three different radii (13.5 μm, 22 μm, and 31 μm). The value of hematocrit

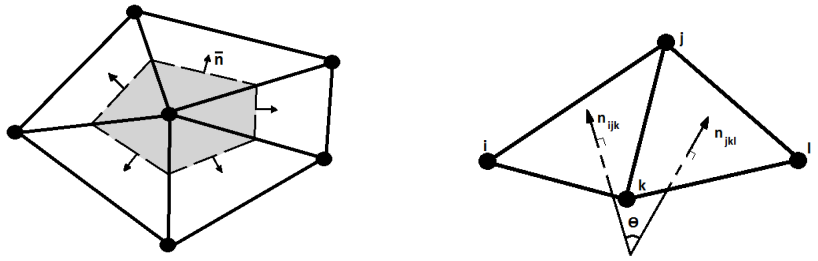

(a) (b)

Figure 1. The control area of a particle (a). Two neighbouring triangular elements of the erythrocyte membrane (b).

in simulations was around 45%, which corresponds to the real hematocrit value of blood.

1. Erythrocyte model

The RBC model described here is based on the description of its membrane. An RBCs' membrane includes a lipid bilayer and the spectrin network connected by transmembrane proteins [26]. Such membrane exhibits incompressible properties, resistance to areal changes and planar shear deformation. The membrane is represented as a two-dimensional network of particles. Due to the elasticity of the RBCs' membrane, the membrane particles are connected by springs (modelled by Hooke's law) to form an irregular polyhedron with triangular sides. Forces acting upon the membrane particles are chosen similarly to [17]. The first force acts between any two neighbouring vertices and describes the ability of the corresponding joint to elongate:

$$\mathbf{F}_s = k_s \left(1 - \frac{l}{l_0}\right) l_c \tau \tag{1.1}$$

where l is the length of the joint between two vertices, l_0 is the equilibrium length, k_s is the stiffness coefficient, and τ is the unit vector, which is codirectional with the vector connecting two neighbouring particles.

To express the areal incompressibility, the force resisting any change in the triangular element area is introduced:

$$\mathbf{F}_a = k_a \left(1 - \frac{s}{s_0}\right) l_c \mathbf{n} \tag{1.2}$$

where s is the area of the triangular element, s_0 is the equilibrium area, k_a is the area expansion modulus, l_c is the length of the side of the control area for the particle, which is shown in Fig. 1a, and $\mathbf{n}$ is the unit vector normal to this side. Such force appears in a particle from all triangle elements sharing this particle.

Since the out-of-plane bending deformation is present in the RBC behavior, bending springs are introduced between each two neighbouring triangular elements:

$$\mathbf{F}_{b_i} = k_b \tan\left(\frac{\theta}{2}\right) \mathbf{n}_{ijk} \tag{1.3}$$

$$\mathbf{F}_{b_l} = k_b \tan\left(\frac{\theta}{2}\right) \mathbf{n}_{jkl} \tag{1.4}$$

$$\mathbf{F}_{b_j} = \mathbf{F}_{b_k} = -\frac{\mathbf{F}_{b_i} + \mathbf{F}_{b_l}}{2} \tag{1.5}$$

where θ is the angle between the neighbouring triangular elements, k_b is the stiffness coefficient, $\mathbf{n}_{ijk}$ and $\mathbf{n}_{jkl}$ are the unit vectors normal to the corresponding triangles (see Fig. 1b, $\mathbf{F}_{b_i}$, $\mathbf{F}_{b_j}$, $\mathbf{F}_{b_k}$, and $\mathbf{F}_{b_l}$ are the forces that act on the particles with the numbers i, j, k, and l respectively, as a result of the change in the angle between two neighbouring triangles that contain these particles. Similar forces act on the particles from each pair of the neighbouring triangles. A tangential function is chosen to avoid the folding of the spring under a large bending deformation [39].

So far, only membrane characteristics have been described, which alone does not ensure the RBC shape. In order to obtain its shape, an additional type of force is needed to describe the volume surrounded by the shell, i.e. the volume of the erythrocyte. Hence, a fourth force which acts upon the triangular element is introduced:

$$\mathbf{F}_v = k_v \left(1 - \frac{v}{v_0}\right) s\mathbf{n} \tag{1.6}$$

where v is the polyhedron volume, v_0 is the relaxation volume, and k_v is the coefficient which is equivalent to the bulk modulus, s is the area of the triangular element and $\mathbf{n}$ is the unit normal vector to this triangle.

An erythrocyte is known to be deformable and easily changing in shape under the influence of external forces. However, in a healthy erythrocyte the area of its membrane, as well as its volume remains almost constant. Therefore, the stiffness coefficients in the model are chosen correspondingly. The values k_v and k_a are larger making the membrane more resistant to changes in its area, while k_s is lower to allow for the shape changes. The typical values of the parameters which we use in simulations are as follows: $k_s = 0.4 \cdot 10^{-11}$ N, $k_a = 5 \cdot 10^{-4}$ N/m, $k_v = 2\,\mathrm{N/m^2}$, $k_b = 2.4 \cdot 10^{-11}$ N. They are similar to the values used in the literature [18, 39]. The equilibrium length of the intervals between the particles, the triangle element area, and the relaxation volume of erythrocytes are: $l_0 = 5.53 \cdot 10^{-7}$ m, $s_0 = 1.45 \cdot 10^{-13}\,\mathrm{m^2}$, $v_0 = 2.66 \cdot 10^{-16}\,\mathrm{m^3}$, respectively. The mesh for each erythrocyte consists of 1280 triangles.

In order to prevent cell penetration between cells, we use the soft contact algorithm [4].

2. Platelet model

The model of a platelet is similar to the erythrocyte model. Platelets are small cells, 2–3 μm in diameter, that do not have a nucleus. We consider a platelet as an elastic membrane that consists of particles connected by springs. The forces acting on each particle are described by equations (1.1)–(1.6). We chose the same parameters values for forces acting in a platelet as for erythrocytes. The equilibrium length of the intervals between the particles, the triangle element area, and the relaxation volume of platelets were: $l_0 = 6.18 \cdot 10^{-7}$ m, $s_0 = 1.65 \cdot 10^{-13}$ m^2, $v_0 = 3.65 \cdot 10^{-18}$ m^3, respectively. The mesh for each platelet consisted of 80 triangles. The difference in the relaxation volume between the platelets and the erythrocytes crucially affects the behaviour of cells. The value of v_0 for erythrocytes was about 0.6 of the volume of a sphere that is composed by elements with the given equilibrium joint length and triangle area, whereas the value of v_0 for platelets was just the volume of a sphere corresponding to the equilibrium parameters. As a result, the platelets remain almost spherical or ellipsoidal in their shape, while the erythrocytes acquire their specific biconcave shape.

3. Modelling flow

We use the Dissipative Particle Dynamics (DPD) method in the form described in the literature [11, 15, 19]. It is a mesoscale method, meaning that each DPD particle describes some small volume of a simulated medium rather than an individual molecule. The method is governed by three equations describing the conservative, dissipative and random forces acting between each two particles:

$$\mathbf{F}^C_{ij} = F^C_{ij}(r_{ij})\hat{\mathbf{r}}_{ij} \tag{3.1}$$

$$\mathbf{F}^D_{ij} = -\gamma\omega^D(r_{ij})(\mathbf{v}_{ij}\cdot\hat{\mathbf{r}}_{ij})\hat{\mathbf{r}}_{ij} \tag{3.2}$$

$$\mathbf{F}^R_{ij} = \sigma\omega^R(r_{ij})\frac{\xi_{ij}}{\sqrt{\Delta t}}\hat{\mathbf{r}}_{ij} \tag{3.3}$$

where $\mathbf{r}_i$ is the vector of the position of the particle i, $\mathbf{r}_{ij} = \mathbf{r}_i - \mathbf{r}_j$, $r_{ij} = \left|\mathbf{r}_{ij}\right|$, $\hat{\mathbf{r}}_{ij} = \mathbf{r}_{ij}/r_{ij}$, and $\mathbf{v}_{ij} = \mathbf{v}_i - \mathbf{v}_j$ is the difference between the velocities of two particles, Δt is the time step in simulations, γ and σ are the coefficients which determine the strength of the dissipative and the random force, respectively, while ω^D and ω^R are weight functions; ξ_{ij} is a normally distributed random variable with zero mean, unit variance, and $\xi_{ij} = \xi_{ji}$. The conservative force is given by the equality

$$F^C_{ij}(r_{ij}) = \begin{cases} a_{ij}(1 - r_{ij}/r_c), & r_{ij} \leqslant r_c \\ 0, & r_{ij} > r_c \end{cases} \tag{3.4}$$

where a_{ij} is the conservative force coefficient between the particles i and j, and r_c is the cut-off radius.

Each of the forces is applied to the fluid particles, as well as to the particles constituting RBC and platelet membranes.

The random and dissipative forces form a thermostat. If the following two relations are satisfied, the system will preserve its energy and maintain the equilibrium temperature:

$$\omega^D(r_{ij}) = \left[\omega^R(r_{ij})\right]^2, \qquad \sigma^2 = 2\gamma k_B T \tag{3.5}$$

where k_B is the Boltzmann constant and T is the temperature. The weight functions are determined by:

$$\omega^R(r_{ij}) = \begin{cases} (1 - r_{ij}/r_c)^k, & r_{ij} \leqslant r_c \\ 0, & r_{ij} > r_c \end{cases} \tag{3.6}$$

where $k = 1$ for the original DPD method, but it can be also varied in order to change the dynamic viscosity of the simulated fluid [11]. The motion of particles is determined by Newton's second law of motion:

$$\begin{aligned} \Delta \mathbf{r}_i &= \mathbf{v}_i \Delta t \\ \Delta \mathbf{v}_i &= \frac{\Delta t}{m_i} \sum_{j \neq i} \left(\mathbf{F}_{ij}^C + \mathbf{F}_{ij}^D + \mathbf{F}_{ij}^R \right), \end{aligned} \tag{3.7}$$

where m_i is the mass of the particle i.

The Euler method or a modified version of the velocity-Verlet method [1, 15], which is more accurate, can be used to integrate equations (3.7). In the former,

$$\mathbf{v}_i^{n+1} = \mathbf{v}_i^n + \frac{1}{m_i} \mathbf{F}_i \left(\mathbf{r}_i^n, \mathbf{v}_i^n \right) \Delta t \tag{3.8}$$

$$\mathbf{r}_i^{n+1} = \mathbf{r}_i^n + \mathbf{v}_i^{n+1} \Delta t \tag{3.9}$$

where indices n and $n+1$ denote the time steps, and

$$\mathbf{F}_i = \sum_{j \neq i} \left(\mathbf{F}_{ij}^C + \mathbf{F}_{ij}^D + \mathbf{F}_{ij}^R \right). \tag{3.10}$$

The discretization in the second method is as follows:

$$\mathbf{r}_i^{n+1} = \mathbf{r}_i^n + \mathbf{v}_i^n \mathrm{d}t + \frac{1}{2} \mathbf{a}_i^n \Delta t^2 \tag{3.11}$$

$$\mathbf{v}_i^{n+1/2} = \mathbf{v}_i^n + \frac{1}{2} \mathbf{a}_i^n \Delta t \tag{3.12}$$

$$\mathbf{a}_i^{n+1} = \frac{1}{m_i} \mathbf{F}_i \left(\mathbf{r}_i^{n+1}, \mathbf{v}_i^{n+1/2} \right) \tag{3.13}$$

$$\mathbf{v}_i^{n+1} = \mathbf{v}_i^{n+1/2} + \frac{1}{2} \mathbf{a}_i^{n+1} \Delta t \tag{3.14}$$

where a_i^n denotes the acceleration of the particle i at the n^{th} time step. Both methods give close results.

The following values of the parameters were used: $r_c = 1 \cdot 10^{-6}$ m, $a_{i,j} = 1 \cdot 10^{-12}$ N, $\gamma = 1 \cdot 10^{-8}$ kg·sec/m^4, $\sigma = 1 \cdot 10^{-11}$ kg/(m$^3 \cdot \sqrt{\text{sec}}$).

The behaviour of the DPD method, as well as its suitability for the problem of fluid simulation is extensively described in the literature [11, 13, 15, 19, 33]. In [11, 13] DPD simulation results are compared to the results obtained by using continuous methods (Navier–Stokes and Stokes equations) for Couette, Poiseuille, square-cavity and triangular-cavity flow.

Let us note that in order to have a nonzero velocity field, we should apply either nonzero flow velocity at the entrance of the domain or a volume force in the whole domain. These two approaches are basically equivalent, though some difference may appear in non-cylindrical domains. Numerical simulations show that this difference is not essential for the results presented here. We have used the approach with the volume force in our simulations.

The simulations were carried out in a cylindrical channel. The no-slip boundary condition at the cylinder wall and the periodical boundary condition in the direction of the cylinder axis were used.

4. Results

Numerical simulations were carried out for the following parameters. The radius R of the cylindrical channel was set to 13.5, 22 or 31 μm, its length was chosen in such a way that it did not influence the results. Usually, it is sufficient to take $L = 2R$. The erythrocytes fill 43–45% of the total volume. This corresponds to the normal hematocrit level in blood. The number of erythrocytes was from 80 to 300 depending on the radius of the cylinder.

The initial erythrocyte location is shown in Fig. 2. The proportion of platelets is greater than in the normal blood. This accelerates their redistribution in the flow and reduces the computational time. However, this does not practically influence their steady distribution.

The volume force applied to the fluid is 10000 N/kg. In this case we obtain the average flow velocity equal to 0.1 mm/s for $R = 13.5$ μm and 0.5 mm/s for $R = 31$ μm. The effective viscosity is $4 - 5 \cdot 10^{-3}$ Pa·s. The corresponding viscosity of the homogeneous fluid (without blood cells) is $1.8 - 2 \cdot 10^{-3}$ Pa·s. These values correspond to the experimental values of blood viscosity. The wall shear rate is equal to 60 sec^{-1} for $R = 13.5\mu$m, 80 sec^{-1} for $R = 22\mu$m and 230 sec^{-1} for $R = 31\mu$m.

The snapshots of the numerical simulations are shown in Fig. 3 (some parts of the computational domains). In order to obtain a steady cell distribution over the cross-section of the channel, the simulations continued at least 5–10 seconds of physical time for $R = 13.5\mu$m and at least 30–50 seconds for $R = 31\mu$m.

In order to determine the cells distribution in the cross-section of the cylinder, we divided it into n narrow annuli S_i for which $r_i < r < r_{i+1}$, $r_0 = 0$, $r_n = R$. We counted the number N_i of the cells' vertices belonging to each annulus during some sufficiently large time T. Next, we divide N_i by the area of the corresponding annulus S_i. We call this ratio the cell distribution in the cross-section and denote it by D.

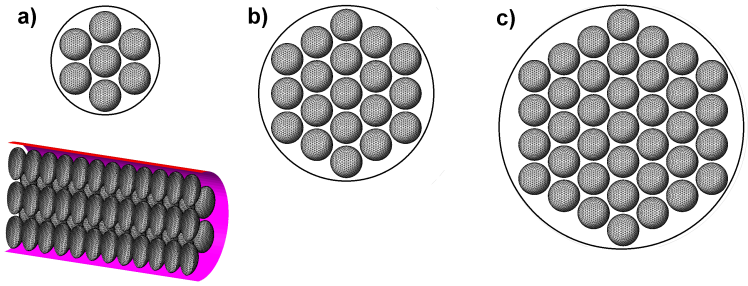

Figure 2. Cross-sections of cylindrical channels and initial erythrocyte positions for different channel radii: (a) 13.5 μm, (b) 22 μm, and (c) 31 μm. Below: (a) an image of an intersection along flow axis shows the length of the simulated channel, as well as the initial placement of RBCs.

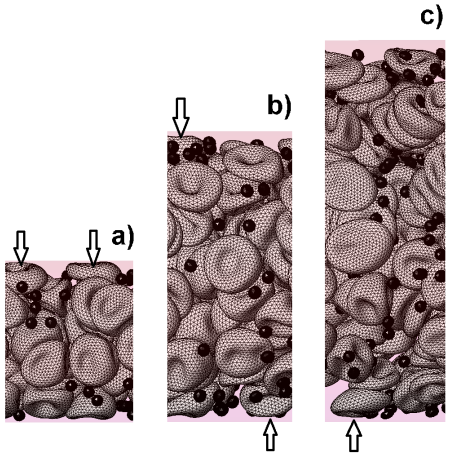

Figure 3. Snapshots of numerical simulations showing RBCs and platelets in cylindrical channels for three different channel radii: (a) 13.5 μm, (b) 22 μm, and (c) 31 μm. RBCc are modelled as elastic highly deformable membranes, while platelets are modelled as elastic membranes which remain approximatively spherical in shape. Blood plasma particles, which occupy the remaining volume of the channel, are not shown on the snapshots.

The distribution curves scaled by their maximum are shown in Fig. 4.

Figure 4a shows the erythrocyte distribution in the cross-section of a cylinder for different values of its radius. Their concentration gradually increases toward the axis. However, it is possible that some erythrocytes are pushed to the boundary and stay trapped there during some time. Examples of such pushed cells are shown in Fig. 3 and marked by arrows. The local maxima near the wall in Fig. 4 are related to this effect, the width of the peaks is comparable to the width of an erythrocyte.

Figure 4b shows the distributions of platelets in the same simulations. In all cases, there is a strong increase in their particle number near the wall. This corresponds to experimental observations [20]. When we increase the radius of the channel, another maximum of the concentration appears near the axis. It is particularly visible for $R = 31\mu$m (solid curve).

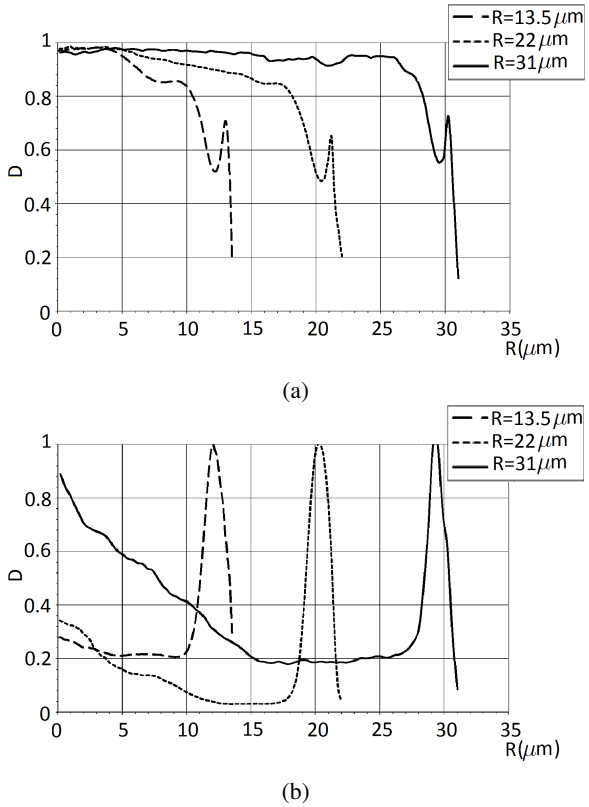

Figure 4. Erythrocyte (a) and platelet (b) distribution as a function of the distance from the flow axis for three channels with different radii: 13.5 μm (long dashed line), 22 μm (short dashed line), and 31 μm (solid line).

Figure 5 shows the averaged velocity profiles in simulations with erythrocytes and platelets.

Conclusion

In this paper we have presented a numerical model and numerical simulations of three-dimensional hemodynamics based on the particle methods for the description of blood plasma, red blood cells and platelets. Using the combination of the spring network model for cells and the DPD method for plasma, we obtain a realistic description of the blood flow. This study illustrates such well-known effects as the RBCs migration to the vessel axis and near-wall magrination of the platelets in the blood flow. Platelets are pushed to the vessel walls by erythrocytes. It is an important mechanism involved in blood coagulation.

The method used in this work has some limitations. In particular, they concern the simplified description of the blood cells. In reality they have a more complex

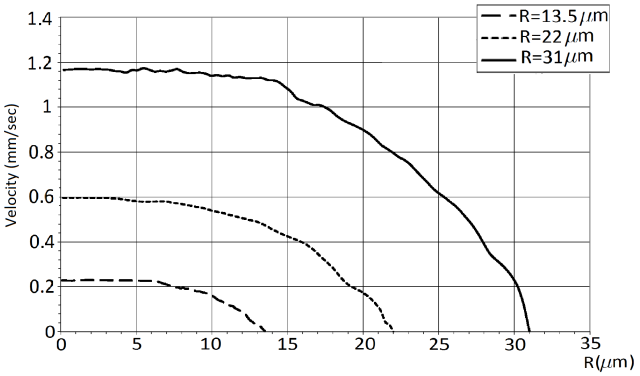

Figure 5. Averaged velocity profiles in simulations with erythrocytes and platelets. Velocity profiles are shown as functions of the distance from the flow axis for three channels with different radii: 13.5 μm (long dashed line), 22 μm (short dashed line), and 31 μm (solid line).

structure than in the model and they can interact with each other forming aggregates. Furthermore, we do not take into account the elastic properties of the vessel walls. Another limitation is related to computational time. We can only consider microvessels, because simulations are quite expensive from the computational point of view.

In spite of these limitations, the simulations described above can now be used to investigate various biomedical issues. For example, thrombosis and hemostasis are very important and challenging issues which need detailed modelling and simulation. This modelling can also be applied in diagnosing various diseases, such as leukemia that can change the mechanical properties of blood cells. Another interesting question is the simulation of the blood flow in vessels with a complex geometry. These aspects will be studied in the forthcoming works.

References

1. M. P. Allen and D. J. Tidesley, *Computer Simulation of Liquids*. Clarendon, Oxford, 1987.
2. T. AlMomani, H. S. Udaykumar, J. S. Marshall, and K. B. Chandran, Micro-scale dynamic simulation of erythrocyte-platelet interaction in blood flow. *Annals Biomed. Engrg.* (2008) **36**, No. 6, 905–920.
3. P. Bagchi, Mesoscale simulation of blood flow in small vessels. *Biophysical J.* (2007) **92**, No. 6, 1858–1877 (PubMed: 17208982).
4. N. M. Bessonov, S. F. Golovashchenko, and V. A. Volpert, Numerical modelling of contact elastic-plastic flows. *Math. Model. Natur. Phenom* (2009) **4**, 44–87.
5. C. Bui, V. Lleras, and O. Pantz, Dynamics of red blood cells in 2D. ESAIM Proc., 2009, Vol. 28, pp. 182–194.
6. L. M. Crowl and A. L. Fogelson, Computational model of whole blood exhibiting lateral platelet motion induced by red blood cells. *Int. J. Numer. Method. Biomed. Engrg.* (2010) **26**, No. 3-4, 471–487.
7. M. M. Dupin, I. Halliday, C. M. Care, L. Alboul, and L. L. Munn, Modelling the flow of dense

suspensions of deformable particles in three dimensions. *Physical Review E* (2007) **75**, 066707.

8. W. Dzwinel, K. Boryczko, and D. A. Yuen, Modelling mesoscopic fluids with discrete-particles methods. Algorithms and results. In: *Finely Dispersed Particles: Micro-, Nano-, and Atto-Engineering* (Eds. A. M. Spasic and J. P. Hsu). Taylor&Francis, CRC Press, pp. 715–778.
9. D. Fedosov, B. Caswell, and G. E. Karniadakis, *General Coarse-Grained Red Blood Cell Models: I. Mechanics*. arXiv:0905.0042 (q-bio.CB) 2009.
10. D. Fedosov, B. Caswell, and G. E. Karniadakis, A Multiscale red blood cell model with accurate mechanics, rheology, and dynamics. *Biophys. J.* (2010) **98**, 2215–2225.
11. D. A. Fedosov, Multiscale modelling of blood flow and soft matter. *PhD Thesis*, Brown University, 2010.
12. D. A. Fedosov, H. Lei, B. Caswell, S. Suresh, and G. E. Karniadakis, Multiscale modelling of red blood cell mechanics and blood flow in malaria. *PLoS Comput. Biology* (2011) **7**, No. 12, e1002270.
13. D. A. Fedosov, I. V. Pivkin, and G. E. Karniadakis, Velocity limit in DPD simulations of wall-bounded flows. *J. Comp. Phys.* (2008) **227**, 2540–2559.
14. H. L. Goldsmith and V. T. Turitto. Rheological aspects of thrombosis and haemostasis: basic principles and applications. *Thrombosis and Haemostasis* (1986) **55**, No. 3, 415–435.
15. R. D. Groot and P. B. Warren, Dissipative particle dynamics: bidging the gap between atomistic and mesoscopic simulation. *J. Chem. Phys.* (1997) **107**, No. 11, 4423–4435.
16. S. M. Hosseini and J. J. Feng, A particle-based model for the transport of erythrocytes in capillaries. *Chem. Engrg. Sci.* (2009) **64**, 4488–4497.
17. Y. Imai, H. Kondo, T. Ishikawa, C. T. Lim, and T. Yamaguchi, Modelling of hemodynamics arising from malaria infection. *J. Biomechanics* (2010) **43**, 1386–1393.
18. Y. Imai, K. Nakaaki, H. Kondo, T. Ishikawa, C. T. Lim, and T. Yamaguchi, Margination of red blood cells infected by plasmodium falciparum in a microvessel. *J. Biomechanics* (2011) **44**, 1553–1558.
19. M. Karttunen, I. Vattulainen, and A. Lukkarinen, *A Novel Methods in Soft Matter Simulations*. Springer, Berlin, 2004.
20. J. F. Koleski and E. C. Eckstein, Near wall concentration profiles of 1.0 and 2.5 μm beads during flow of blood suspensions. *Trans. Ann. Soc. Intern. Organs* (1991) **37**, 9–12.
21. P. W. Kuchel and E. D. Fackerell, Parametric-equation representation of biconcave erythrocytes. *Bulletin Math. Biology* (1999) **61**, 209–220.
22. R. C. Leif and J. Vinograd, The distribution of buoyant density of human erythrocytes in bovine albumin solutions. *Proc. Nat. Acad. Sci. USA* (1964) **51**, No. 3, 520–528.
23. S. Leibler and A. C. Maggs, Simulation of shape changes and adhesion phenomena in an elastic model of erythrocytes. *Proc. Nat. Acad. Sci. USA* (1990) **87**, 6433–6435.
24. L. Lopez, I. M. Duck, and W. A. Hunt, On the shape of the erythrocyte. *Biophys J.* (1968) **8**, No. 11, 1228–1235.
25. J. L. McWhirter, H. Noguchi, and G. Gompper, Flow-induced clustering and alignment of vesicles and red blood cells in microcapillaries. *PNAS* (2009) **106**, No. 15, 6039–6043.
26. N. Mohandas and P. G. Gallagher, Red cell membrane: past, present, and future. *Blood* (2008) **112**, 3939–3948.
27. L. L. Munn and M. M. Dupin, Blood cell interactions and segregation in flow. *Annals Biomed. Engrg.* (2008) **36**, No. 4, 534–544.

28. S. Muñoz San Martín, J. L. Sebastián, M. Sancho1, and G. Álvarez, *Modelling Human Erythrocyte Shape and Size Abnormalities*. arXiv:q-bio/0507024 [q-bio.QM], 2005.

29. H. Noguchi and G. Gompper, Shape transitions of fluid vesicles and red blood cells in capillary flows. *PNAS* (2005) **102**, No. 40, 14159–14164.

30. D. Obrist, B. Weber, A. Buck, and P. Jenny, Red blood cell distribution in simplified capillary networks. *Phil. Trans. R. Soc. A* (2010) **368**, doi: 10.1098/rsta.2010.0045.

31. I. V. Pivkin and G. E. Karniadakis, Accurate coarse-grained modelling of red blood cells. *Phys. Review Letters, PRL 101* (2008) 118105.

32. C. Pozrikidis, *Modelling and Simulation of Capsules and Biological Cells*. Chapman&Hall/CRC, 2003.

33. U. D. Schiller, Dissipative particle dynamics. A study of the methodological background. *Diploma Thesis*, Faculty of Physics University of Bielefeld, 2005.

34. R. Skalak, A. Tozeren, R. Zarda, and S. Chein, Strain energy function of red blood cell membranes. *Biophys. J.* (1973) **13**, No. 3, 245–264 (PubMed: 4697236).

35. A. A. Tokarev, A. A. Butylin, F. I. Ataullakhanov, Platelet adhesion from shear blood flow is controlled by near-wall rebounding collisions with erythrocytes. *Biophys. J.* (2011) **100**, No. 4, 799–808.

36. A. A. Tokarev, A. A. Butylin, and F. I. Ataullakhanov. Platelet transport and adhesion in shear blood flow: The role of erythrocytes. *Computer Research Modelling* (2012) **4**, No. 1, 185–200 (in Russian).

37. A. A. Tokarev, A. A. Butylin, E. A. Ermakova, E. E. Shnol, G.P. Panasenko, and F. I. Ataullakhanov, Finite platelet size could be responsible for platelet margination effect. *Biophysical J.* (2011) **101**, 1835–1843.

38. A. Tosenberger, V. Salnikov, N. Bessonov, E. Babushkina, and V. Volpert, Particle dynamics methods of blood flow simulations. *Math. Model. Nat. Phenom.* (2011) **6**, No. 5, 320–332.

39. K. Tsubota and S. Wada, Elastic force of red blood cell membrane during tank-treading motion: Consideration of the membrane's natural state. *J. Mechan. Sci.* (2010) **52**, 356–364.

40. K. Tsubota, S. Wada, H. Kamada, Y. Kitagawa, R. Lima, and T. Yamaguchi, A particle method for blood flow simulation, application to flowing red blood cells and platelets. *J. Earth Simul.* (2006) **5**, 2–7.

41. C. Yeh, A. C. Calvez, and E. C. Eckstein, An estimated shape function for drift in a platelet-transport model. *Biophys. .* (1994), **67**, 1252–1259.

42. C. Yeh and E. C. Eckstein, Transient lateral transport of platelet-sized particles in flowing blood suspensions. *Biophys. J.* (1994) **66**, 1706–1716.

43. J. Zhang, P. C. Johnson, and A. S. Popel, Effects of erythrocyte deformability and aggregation on the cell free layer and apparent viscosity of microscopic blood flows. *Microvasc Res.* (2009) **77**, No. 3, 265–272.